On the Dynamics of the Coupled Mixed Layer-Thermocline System and the Determination of the Oceanic Surface Density[1]

JOSEPH PEDLOSKY

Woods Hole Oceanographic Institution, Woods Hole, MA 02543

WENDY SMITH

WHOI/MIT Joint Program

J. R. LUYTEN

Woods Hole Oceanographic Institution, Woods Hole, MA 02543

(Manuscript received 29 February 1984, in final form 4 May 1984)

ABSTRACT

A simple model of the oceanic mixed layer is coupled to a model of the ventilated thermocline. The model allows a combination of advection and surface heating to determine the position of the outcrop lines of the isopycnals. The resulting isopycnal outcrops determine the circulation in the ventilated thermocline as in the 1983 study by Luyten, Pedlosky and Stommel (LPS). The isopycnal outcrop line is affected by both Ekman wind drift and the surface geostrophic flow. Hence, the outcrop position and the thermocline circulation are coupled.

The mixed layer and the thermocline models are extremely simple. Each is modeled by layers of constant density. The mixed layer, in which the isopycnals are vertical, is distinguished by the ability of fluid to cross the interfaces between adjacent layers under the influence of atmospheric heating. The heating is parameterized in terms of the departure of the isopycnal line from the position it would have if the ocean were heated, but at rest.

Although in most major respects the thermocline circulation is qualitatively similar to the model of LPS, the effect of the variation of the outcrop latitude with longitude introduces the possibility of potential-vorticity minima along latitude circles.

The model also predicts cooling of the most southern portion of the subtropical gyre under the influence of northward Ekman wind drift.

1. Introduction

Most analytic theories of the oceanic thermocline take as a starting point a prescribed surface distribution of temperature or density. The resulting density and velocity fields below the surface are sought as consequences of the internal dynamics of the modeled ocean. The prescription of the surface density field is mathematically self-consistent and logically acceptable, but its chief virtue is the simplification it provides for the remaining aspects of the problems of the thermocline.

In fact, it is much more likely that surface heating of the ocean combines with lateral advection of temperature to determine the surface density field; therefore, this determination of the surface density field is coupled to the dynamics of the ocean. Several budget calculations (e.g., Behringer and Stommel,

1981) emphasize the important role of lateral advection on annual (or longer) time scales in the heat balance of the upper mixed layer.

A model of the oceanic thermocline that also possesses the artificial character of a prescribed surface distribution is the recently published, layered model of the ventilated thermocline (Luyten, Pedlosky and Stommel, 1983, hereafter LPS). The model, however, is so simple mathematically that it clearly is a likely candidate for marriage to a similarly simple model of the upper mixed layer so that their joint influence in determining the surface-density field can be assessed and the resulting influence on the thermocline structure determined.

The purpose of this paper is to present an analysis of a simple coupled mixed layer-thermocline model. The central physical simplification comes from carrying the layered representation of the oceanic thermocline into the region of the upper mixed layer. Fig. 1 shows a schematic of the basic idea. Beneath a mixed layer of depth d, the ocean is represented by a series of layers, each of constant density. The
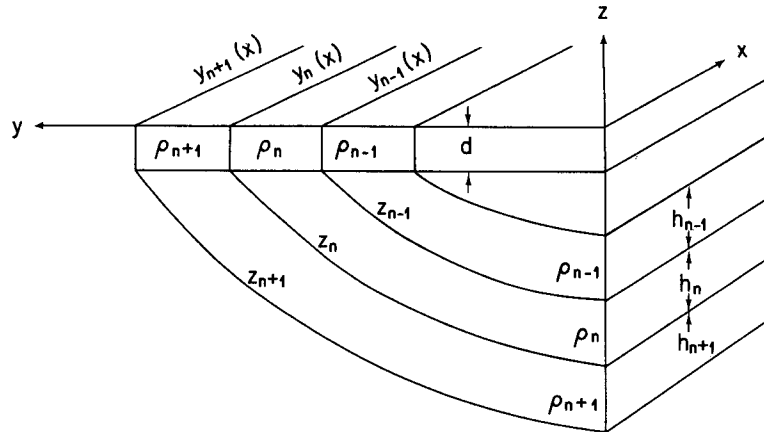
FIG. 1. A schematic of the combined thermocline–mixed layer model. The thermocline consists of layers each of thickness h_n with uniform density ρ_n. The interface z_n between the nth and the $n + 1$st layer hits the base of the mixed layer at the outcrop line $y_n(x)$. The interface is vertical in the mixed layer.

thickness and depth of each layer represent the thermocline structure resolved by the layered model. One basic presumption of the model is that in the region below the mixed layer no fluid crosses the interface between isopycnal layers. The layers are stacked so that heavy fluid underlies lighter fluid, i.e., $\rho_n < \rho_{n+1}$ in this region. On the other hand, the model mixed layer is characterized by vertical isopycnals, i.e., the absence of a vertical density gradient. The interface between the nth and $n + 1$st layer at depth z_n strikes the base of the mixed layer at latitude y_n and then rises vertically to the sea surface. The mixed layer is characterized as a surface zone of depth d in which fluid may cross isopycnal surfaces laterally in response to surface heating.

The goal of the present paper is to formulate a model that can describe such cross-isopycnal flow, determine the outcrop lines y_n (which are generally functions of longitude x) and simultaneously predict the resulting thermocline structure. We leave to the next section a detailed description of the model, but it must be apparent already that progress on this difficult problem will require several idealizations and restrictions. Chief among the latter will be the restriction of our attention to the subtropical gyre where the Ekman pumping velocity is downward. In such situations there will be "detrainment" of the fluid from the mixed layer into the region below, and it is sensible to prescribe continuity of density between the mixed layer and the geostrophic region beneath it; this situation is the one sketched in Fig. 1. For steady states, to which the present theory is also limited, the detrainment velocity is simply the Ekman pumping (de Szoeke, 1980). Since the fluid enters the geostrophic deep layers from the mixed layer in the subtropical gyre, it is precisely in this region where the coupling between the two domains is expected to be strongest.

2. The model

First consider the region of the mixed layer. We take as our starting point a slab model of the mixed layer (see de Szoeke, 1980, for an excellent discussion of the formulation of the basic mixed layer model) so that the horizontal velocity is assumed to be independent of depth within the mixed layer. The present model is restricted entirely to steady state conditions. That is, we will be formulating a coupled model to describe only the time-averaged thermocline flow and a basic presumption is that a steady state model of the mixed layer is adequate for such a purpose.

In that case, the mass balance for the mixed layer may be written

$$\frac{\partial}{\partial x}(u_n d_n) + \frac{\partial}{\partial y}(v_n d_n) = W_E^{(n)}, \qquad (2.1)$$

where x and y are local Cartesian coordinates directed eastward and northward while u_n and v_n are the respective velocity components in those directions; $W_E^{(n)}$ represents the vertical entrainment velocity at the base of the mixed layer. Labels n refer to the region of the mixed layer between outcrop lines y_{n-1} and y_n in which the mixed layer density is ρ_n and the mixed layer depth is d_n. The depth of the mixed layer d_n may be a function of position. A rigid-lid approximation has been assumed to derive (2.1) so that fluid enters or leaves the mixed layer only through its base.

At this point it is useful to borrow an idea usually applied to the derivation of the appropriate matching conditions at the base of the mixed layer (e.g., see Niiler, 1975). Although Figs. 1 and 2 show the transition between layers as discontinuous, it is useful to consider the interface as the limit of a narrow zone, whose width 2δ tends to zero in the limit $\delta \rightarrow$
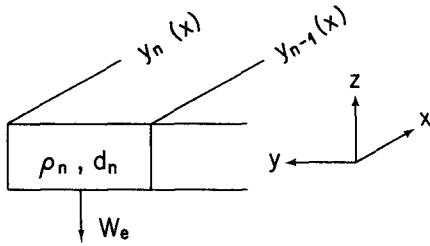
FIG. 2. The slab model of the mixed layer. Between the interfaces $y_{n-1}(x)$ and $y_n(x)$, the mixed layer has depth d_n and density ρ_n. In the subtropical gyre the detrainment velocity W_e is simply the Ekman pumping.

0, in which all the fields are continuous. Thus, Fig. 3 shows the zone, centered on $y_n(x)$, through which the density of the mixed layer changes from ρ_n to ρ_{n+1}.

If (2.1) is integrated in y across this zone, we obtain

$$\frac{\partial}{\partial x} \int_{y_n-\delta}^{y_n+\delta} (u_T d_T) dy + d_{n+1} \left[v_{n+1} - u_{n+1} \frac{dy_n}{dx} \right]$$

$$- d_n \left[v_n - u_n \frac{dy_n}{dx} \right] + \int_{y_n-\delta}^{y_n+\delta} W_{ET} dy = 0, \quad (2.2)$$

where the label T refers to variables in the thin transition zone.

Assuming only that $u_T d_T$ and W_{ET} are finite in the transition zone, it follows from the limit $\delta \rightarrow 0$ that the quantity

$$V_n = d_n \left[v_n - u_n \frac{dy_n}{dx} \right]$$

$$= d_{n+1} \left[v_{n+1} - u_{n+1} \frac{dy_n}{dx} \right] \quad (2.3)$$

is continuous across the outcrop line. Here V_n is the lateral entrainment of volume per unit time per unit length along the outcrop line. If V_n were zero, fluid in the mixed layer would flow entirely parallel to the outcrop line. If V_n is negative, fluid crosses the interface between isopycnal regions such that fluid of density ρ_{n+1} becomes fluid of density ρ_n. If $\rho_n < \rho_{n+1}$, this implies the existence of external heating in the transition zone to accomplish this transformation.

To examine this further, consider the equation for thermal energy conservation applied to the mixed layer. In a steady state where there is no entrainment of colder fluid from beneath the mixed layer (recall, in the present case there is only detrainment with, consequently, no temperature jump at the base of the mixed layer), the heat balance is simply

$$d_n u_n \frac{\partial T_n}{\partial x} + d_n v_n \frac{\partial T_n}{\partial y} = Q_n, \quad (2.4)$$

where T_n is the temperature of the mixed layer fluid of density ρ_n, and Q_n is the surface heat flux into the mixed layer from the atmosphere.

Now consider (2.4) integrated over the transition zone shown in Fig. 3. It directly follows from (2.1), (2.3) and (2.4) that

$$\frac{\partial}{\partial x} \int_{y_n-\delta}^{y_n+\delta} (duT)_T dy + V_n(T_{n+1} - T_n) = \int_{y_n-\delta}^{y_n+\delta} Q_T dy, \quad (2.5)$$

where, again, the label T refers to variables continuously defined in the transition zone. In the limit $\delta \rightarrow 0$, the first term on the left-hand side of (2.5) vanishes if, as before, we assume that duT is bounded in the zone as $\delta \rightarrow 0$. Thus (2.5) becomes

$$V_n(T_{n+1} - T_n) = Q_n \equiv \lim_{\delta \rightarrow 0} \int_{y_n-\delta}^{y_n+\delta} Q_T dy. \quad (2.6)$$

If we examine (2.4) and (2.5) together, an inconsistency superficially appears unavoidable. If the density and temperature are laterally uniform between y_n and y_{n+1}, then the left-hand side of (2.4) becomes identically zero. At the same time, in order for fluid to pass across the outcrop line $y_n(x)$, a nonzero value of Q_n is necessary. This inconsistency is only apparent, rather than real, because the use of a horizontally layered model of the mixed layer implies that the net surface heat flux should be regarded as concentrated and limited to an input entirely in the transition zone whose strength Q_n represents the heating required for the finite density transformation of the layered model. Thus, in this model the heating is imagined limited to the transition zone and has a nonzero integral across that zone and we must realize that this lumping of the applied heating at the outcrop line is the layered representation of what is, in fact, a continuous process of incremental temperature transformations as the fluid moves laterally through a continuous horizontal density gradient.

The next important step is the specification of the heating function Q_n. Consider the situation that would arise if the ocean was at rest and was being heated by the atmosphere. In the steady state, the
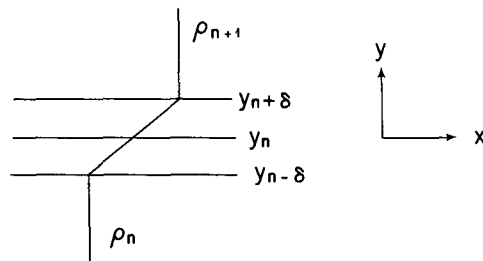

FIG. 3. An enlargement of the lateral transition zone between two constant density regions. We are interested in the limit $\delta \rightarrow 0$.

ocean surface temperature would match the atmospheric sea-level temperature and the heat flux between the two would cease.[2] Suppose that in this state the resulting surface temperature (or density) isolines are given by the equilibrium value

$$y_n = Y_n(x). \qquad (2.7)$$

Now, in the case where the ocean is moving, advection will impose a departure of the outcrop lines y_n from the equilibrium outcrop lines $Y_n(x)$. If the resulting heat exchange with the atmosphere is assumed to be a linear function of the air–sea temperature difference, it suggests writing (2.6) as

$$V_n(T_{n+1} - T_n) = \hat{\kappa}_n[Y_n(x) - y_n(x)], \qquad (2.8)$$

where $\hat{\kappa}_n$ is a "relaxation" coefficient which measures the rate at which the surface isotherms will tend to their at rest ocean values. If $T_{n+1} < T_n$, then, generally, southward flux through the isotherm boundary between region $n + 1$ and region n requires an external heating. From (2.8) this would require the surface isotherm to be advected south of its equilibrium position exposing relatively cooler surface water to be heated by the atmosphere.

With (2.3), (2.8) may be written as

$$\left(v_n - u_n \frac{dy_n}{dx}\right) = -\left[\frac{\hat{\kappa}_n}{d_n(T_n - T_{n+1})}\right](Y_n - y_n),$$

or,

$$v_n - u_n \frac{dy_n}{dx} = -\kappa_n(Y_n - y_n), \qquad (2.9)$$

where

$$\kappa_n \equiv \hat{\kappa}_n/d_n(T_n - T_{n+1}). \qquad (2.10)$$

Note that (2.9) (or at least its form) might be plausibly derived in an alternative fashion directly from the thermal equation for a *continuously* variable surface temperature field. If Q_n in (2.4) is proportional to the air–sea temperature difference so that (2.4) can be modeled as

$$u \frac{\partial T}{\partial x} + v \frac{\partial T}{\partial y} = \kappa(T_a - T), \qquad (2.11)$$

where T_a is the atmospheric surface temperature, then division of (2.11) by $\partial T/\partial y$ yields

$$v - u\left(\frac{\partial y}{\partial x}\right)_T = \frac{\kappa(T_a - T)}{\partial T/\partial y}. \qquad (2.12)$$

Suppose T is "close" to T_a and that the latter is essentially only a function of latitude, then

$$\frac{T_a - T}{\partial T/\partial y} \approx \frac{\partial T_a/\partial y}{\partial T/\partial y}(y - y_a) \approx (y - y_a), \qquad (2.13)$$

which would give (2.12) the same form as (2.9). This argument is only suggested to make the form (2.9) more intuitively acceptable. In the derivation of (2.9) no restriction to small departures of y_n from Y_n is required, nor is Y_n restricted in its longitude dependence.

The form (2.9) is the fundamental equation for the determination of the outcrop isoline for the interface between fluid of densities ρ_n and ρ_{n+1}. The parameter κ_n is an inverse relaxation time for the outcrop to attain its equilibrium position $Y_n(x)$ if the ocean circulation were to be turned off.

In general, (2.9) is a nonlinear differential equation since both u_n and v_n are functions of y and since (2.9) is applied to the line $y = y_n(x)$, (2.9) is in fact

$$u_n(x, y_n) \frac{dy_n}{dx} - v_n(x, y_n) = -\kappa_n(Y_n - y_n), \qquad (2.14)$$

which exposes the nonlinearity explicitly.

The horizontal velocity components, u_n and v_n, each consist of two parts, an Ekman velocity and a geostrophic velocity. The former is simply given by

$$(v_n)_{\text{EKMAN}} = -\tau^{(x)}/\rho_0 f d_n,$$

$$(u_n)_{\text{EKMAN}} = \tau^{(y)}/\rho_0 f d_n, \qquad (2.15)$$

where ρ_0 is the mean density and $\tau^{(x)}$ and $\tau^{(y)}$ are the known eastward and northward components of the applied wind stress. The second component of the velocity field consists of the geostrophic surface velocities. In the layer model these will be the geostrophic velocities in the layer immediately below the outcrop line. That is, to find $y_n(x)$ the geostrophic velocities in the nth layer at the outcrop line must be known or, using the continuity of V_n, the geostrophic velocities in the $n + 1$st layer would also suffice. Since geostrophic velocities in the thermocline region depend sensitively on the position of the outcrop lines, the joint problem of determining $y_n(x)$ and the associated thermocline geostrophic velocities presents a highly coupled nonlinear problem. Surprisingly, the general method of solution presented in the next section is quite straightforward.

3. Method of solution

The key to the solution of the coupled problem described in the previous section is the same as used in LPS. Namely, we consider the zone south of the line $y = y_0$ where the Ekman pumping vanishes (the northern boundary of the subtropical gyre), but north of the first outcrop line $y_2(x)$. In this region there is only one moving layer in which density is ρ_3 and its thickness is h_3. The layer beneath layer 3 is assumed at rest[3]; thus, as shown in LPS,

---

[2] We are here making the sweeping simplification that the complex process of heat exchange, including latent heat, is essentially driven by the air–sea temperature difference.

[3] Pedlosky and Young (1983) describe models in which the deeper, unventilated layers may also be in motion. This only complicates somewhat the method of solution outlined here which can easily be extended to consider such cases.

$$h_3{}^2 = D_0{}^2(x, y) + H_3{}^2, \qquad (3.1)$$

where

$$D_0{}^2 = -\frac{2f^2}{\gamma_3\beta}\int_x^{X_E} W_E(x', y)dx', \qquad (3.2)$$

where β is the planetary vorticity gradient, W_E the Ekman pumping velocity (<0), X_E the position of the eastern boundary and $\gamma_3 = (\rho_4 - \rho_3/\rho_0)g$. The geostrophic zonal velocity is assumed to vanish on the eastern boundary where the depth of the layer is the constant, H_3. With h_3 known, the geostrophic velocities in layer 3 are

$$\left.\begin{aligned}u_3 &= -\frac{\gamma_3}{f}\frac{\partial h_3}{\partial y}\\[2mm] v_3 &= \frac{\gamma_3}{f}\frac{\partial h_3}{\partial x}\end{aligned}\right\}, \qquad (3.3)$$

and are therefore known as functions of x and y.

These geostrophic velocities with the Ekman velocities of (2.10) then allow for the integration of (2.14) to determine the outcrop line. Of course, appropriate initial data must be specified for (2.14), a point we return to below. The more important point is that after $y_2(x)$ has been found, the steady flow in the region $y_1(x) < y < y_2(x)$ can be found by the potential-vorticity trajectory analysis used in LPS so that the geostrophic flow in the domain north of $y_1(x)$ can be determined. With the geostrophic flow in this region now known, (2.14) can then be applied to the determination of $y_1(x)$, after which the geostrophic flow south of $y_1(x)$ can be determined by the method of LPS. It is clear by induction that, in principle, the method can be applied to a model with an arbitrary number of layers and outcrop lines as long as the solutions for $y_n(x)$ do not possess any pathologies such as curling back on themselves and so not spanning the longitude range of the basin. In this paper, largely to demonstrate the basic ideas, we will restrict our attention to the simplest nontrivial case. We will discuss a model with a single outcrop line and determine the flow field both north and south of the line and compare it with the results of a model in which the outcrop line is specified as a latitude circle.

There is one remaining assumption to be discussed and it is an important one. It is clear from (2.15) that the velocities in the upper mixed layer require a knowledge of the mixed layer depth. In principle, mixed layer depth should be treated as an additional unknown. However, it is a little unclear to us precisely how d_n should be determined. According to the argument of de Szoeke (1980), the mixed layer depth is basically determined from a turbulent kinetic-energy balance. If the action of shear-related mixing at the mixed layer base is ignored, and attention is limited to a subtropical detrainment gyre, the equation for d is

$$\overline{\alpha g d_n Q_n} = \overline{2m_0 u_*^3} \qquad (3.4)$$

where an overbar represents an average over each lateral zone. In (3.4) $u_*^2 \equiv |\tau|/\rho_0$, α is the coefficient of thermal expansion and m_0 is an empirical, order-one positive constant. In regions where the surface layer is heated ($Q_n \rightarrow 0$) this fixes d_n as

$$d_n = 2\overline{m_0 u_*^3}/\alpha g \overline{Q_n}, \qquad (3.5)$$

which might be modeled in the layer representation as

$$d_n = 2\frac{\overline{m_0 u_*^3}}{\hat\kappa_n(Y_n - y_n)}(y_{n+1} - y_n), \qquad (3.6)$$

which, of course, tends to complicate an already difficult problem. A more fundamental difficulty arises in that part of the subtropical gyre where the surface waters are being cooled ($Q_n < 0$) in which case (3.4) yields no sensible, steady state prediction for d_n. This situation is likely to occur in the southern part of the subtropical gyre where, under the influence of the trade winds, the stress-driven Ekman transport tends to be northward, driving warm fluid columns northward to be cooled. This is; in fact, what Behringer and Stommel (1981) deduced for their heat budget in the eastern tropical North Atlantic. Quite frankly, we are at a loss to understand how to deal with this important question in a completely deductive fashion. It may well be that a completely steady state model is inadequate for the prediction of mixed layer depth. We will sweep away the real difficulties associated with this vexing question by arbitrarily assigning a mixed layer depth in our model calculations. Although we could assign a spatially variable depth on the basis of observations (e.g., Levitus, 1982), we feel such complexity would be inappropriate to the level of our model. Hence in all our calculations to be presented, the mixed layer depth is a constant.

4. An example

To illustrate the ideas described above, consider the response of an ocean basin to the wind stress directed parallel to latitude circles (i.e., steady zonal) with magnitude

$$\tau = -\rho_0 f\frac{y_0}{\pi} W_0 \cos\frac{\pi y}{y_0}. \qquad (4.1)$$

The region under consideration is

$$0 \leq x \leq a,$$
$$0 \leq y \leq y_0. \qquad (4.2)$$

From (4.1) the Ekman pumping velocity is

$$w_E = -W_0 \sin\frac{\pi y}{y_0}, \qquad (4.3)$$

and if W_0 is positive, the Ekman vertical velocity is negative (downwelling) in the region $0 \leq y \leq y_0$ which we identify with the subtropical gyre.

We consider a model in which there are two moving layers, layers 2 and 3 in Fig. 4 with the ocean at rest beneath layer 3. In layer 3, for $y_2 \leq y \leq y_0$, the application of the Sverdrup transport relation to layer 3, which is the only moving layer in this region yields

$$h_3{}^2 = H_3{}^2 + D_0{}^2(x, y), \qquad (4.4)$$

where

$$D_0{}^2 = \frac{2f^2 a}{\gamma_3 \beta} W_0(1 - x/a) \sin\pi y/y_0 \qquad (4.5)$$

so that the geostrophic components of velocity are, from (3.3),

$$v_3 = -\frac{f}{h_3} \frac{W_0}{\beta} \sin\pi y/y_0,$$

$$u_3 = -\frac{\pi f(a/y_0)}{h_3 \beta} W_0(1 - x/a) \cos\frac{\pi y}{y_0}, \qquad (4.6)$$

while the contribution to the surface velocity field from the Ekman wind-drift currents are given by (2.15), i.e.,

$$(v_3)_{\text{EKMAN}} = \frac{W_0}{\pi} \frac{y_0}{d_3} \cos\frac{\pi y}{y_0},$$

$$(u_3)_{\text{EKMAN}} = 0. \qquad (4.7)$$

It is important to note that in this example, the zonal velocity in (2.14) is entirely the geostrophic component. The meridional component is composed of both the Ekman and geostrophic components. The ratio of the former to the latter is

$$\frac{(v_3)_{\text{EKMAN}}}{v_3} = -\frac{\beta y_0}{\pi f} \frac{h_3}{d_3} \cot\frac{\pi y}{y_0}. \qquad (4.8)$$

If h_3 is $O(H_3)$, then the order of magnitude E of the ratio in (4.8) is given by

$$E = \frac{\beta y_0}{\pi f} \frac{H_3}{d_3}. \qquad (4.9)$$
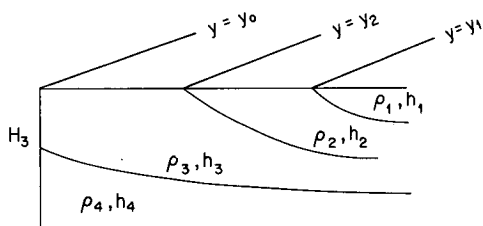

FIG. 4. The domain of the ventilated thermocline. See text for a discussion of the method of solution for the coupled mixed layer-thermocline problem.

Generally, $\beta y_0/f$ is less than unity for the subtropical gyre while H_3/d_3 is typically on the order of 5 to 10. If d_3 is 60 m (which would tend to overestimate E since d_3 for winter seasons is larger), then for y_0/π equal 1000 km, $\beta = 10^{-13}$ cm^{-1} s^{-1} and $f = 10^{-4}$ s^{-1};

$$E = H_3/6, \qquad (4.10)$$

if H_3 is measured in hundreds of meters. Thus, if H_3 is, say, between 400 and 800 m, E is $O(1)$. Of course, as (4.8) shows, the relative importance of the geostrophic and Ekman meridional velocities will depend on position in the gyre. Near the gyre center, $y/y_0 \sim \frac{1}{2}$, the Ekman component will vanish while the dominance of the two components will reverse near the northern and southern gyre boundaries. Thus, a priori both components need to be included in our analysis.

It is also worth noting that in the southern part of the gyre the two meridional components to the velocity will be in opposition and will, in fact, vanish on the line,

$$h_3(x, y) \cot\frac{\pi y}{y_0} = \frac{\pi f d_3}{\beta y_0}. \qquad (4.11)$$

Before using (4.4), (4.6) and (4.7) in (2.14), it is useful to nondimensionalize the variables. Let

$$(x, y) = y_0(x', y'),$$

$$Y = y_0 Y', \qquad (4.12)$$

$$h_3 = H_3 h'_3,$$

then (2.14), with the aid of (4.4), (4.6) and (4.7) becomes

$$(1 - x/b) \cos\pi y \frac{dy}{dx}$$

$$= rh_3(y - Y) + [\sin\pi y - Eh_3 \cos\pi y]/b\pi, \qquad (4.13)$$

where, for simplicity of notation, the primes have been dropped from the dimensionless variables and the subscript 3 is understood to apply to the outcrop line $y(x)$. The dimensionless parameters that appear in (4.13) are

$$
\left.
\begin{aligned}
b &= a/y_0 \\[4pt]
E &= \frac{\beta y_0}{\pi f d_3} H_3 \\[4pt]
r &= \kappa H_3 \beta y_0{}^2/(W_0 f \pi a)
\end{aligned}
\right\} , \qquad (4.14)
$$

while h_3 in (4.13) is given by

$$h_3 = [1 + A(1 - x/b) \sin\pi y]^{1/2}, \qquad (4.15)$$

where

$$A = \frac{2f^2 a W_0}{\gamma_3 \beta H_3{}^2}. \qquad (4.16)$$

The function $Y(x)$ can be arbitrarily specified. In the examples that follow, we will always take Y to be constant. Hence, any departure of $y(x)$ from a latitude circle is due entirely to the interplay between heating and advection.

Before proceeding to the integration of (4.13), some general comments are in order. We have found that it is necessary to integrate (4.13) along the time-like direction in x to achieve numerical stability. That is, for outcrop lines in the northern portion of the gyre, (4.13) will be integrated from west to east. Thus initial data at $x = 0$ are required. This is equivalent to specifying the starting latitude y_W of a surface isopycnal just east of the western boundary current regime. In principle, any y_W is possible, but it seems natural to suppose that a western-boundary current (not included in our model) would tend to advect the surface isopycnals beyond the equilibrium latitude Y. The size of $y_W - Y$ is a measure of the effect of the western-boundary current on the surface density in the western part of the gyre and it is of interest to examine several different values of this parameter.

At the same time, we point out the singularity of (4.13) on the eastern boundary where u_3 vanishes. In all cases that we have considered, we have found that the solution to (4.13) tends, as $x \rightarrow b$, to that value of $y = y_e$ such that $(1 - x/b)dy/dx \rightarrow 0$ as $x \rightarrow b$. That is, at $x = b$ (where $h_3 = 1$), y_e satisfies

$$(\pi b r)^{-1}[\sin \pi y_e - E \cos \pi y_e] + y_e = Y. \quad (4.17)$$

Rather than solve the transcendental equation (4.17), we have reversed the process. We specify y_e and use (4.17) to calculate the equilibrium latitude Y.

For outcrop latitudes in the southern half of the subtropical gyre, the integration proceeds westward from $y = y_e$ at $x = b$. We have not considered cases where the outcrop line crosses from the northern to the southern portion of the gyre.

For large r (i.e., short relaxation times compared to a lateral advection time) (4.13) implies that almost everywhere $y = y_r(x)$, where

$$y_r = Y - r^{-1}[\sin \pi Y - E h_3(x, Y) \cos \pi Y]/$$

$$[\pi b h_3(x, Y)] + O(r^{-2}) \quad (4.18)$$

in the case when Y is constant. Note that for large r, Y and y_e are nearly identical. However, there is no reason why y_W, the starting value for the outcrop line near the western boundary, should satisfy (4.18). As we previously noted, we anticipate $y_W \neq Y$. This implies that in some zone near $x = 0$, the singular perturbation character of (4.13) for large r must be considered. That is, we should anticipate a boundary layer character for $x = O(r^{-1})$ in which the lowest-order balance in (4.13) becomes

$$\cos \pi y \frac{dy}{dx} = r h_3(0, y)(y - Y), \quad (4.19)$$

for which the solution, starting at $x = 0$ with $y = y_W$, will be asymptotic for $x > O(r^{-1})$ to the "interior" solution given by (4.18). As will be seen below, this behavior is also observed for $O(1)$ values of r, i.e., the fairly strong adjustment process in the western side of the basin from the starting value assigned at $x = 0$ to the value predicted by (4.18). Note that for outcrop lines in the northern part of the gyre,

$$y_r < Y,$$

i.e., the outcrop line is swept south of the equilibrium line and this effect is strongest near the eastern boundary where h_3 is smallest, i.e., where the southward geostrophic meridional velocity is greatest.

Implicit in our specification of the coefficients in (4.13) is our use of the β-plane approximation. That is, β and f are considered to be constants where they appear. This slight approximation could be avoided most easily by formulating the original problem in terms of the variables x and f instead of x and y. It seemed to us more desirable at this stage to use the more familiar β-plane formulation.

It is also important to note that (4.13) emphasizes the role the structure of the thermocline has on the form of the outcrop line. In the case where Y is independent of x, then, given the fact that the meridional Ekman velocity is x-independent, the x-variation of the right-hand side of (4.13) depends entirely on the longitudinal variation of the thermocline depth h_3. (Of course, this fact results from our assumption that the mixed layer has a uniform depth.) If h_3 were independent of x, a possible solution of (4.13) would be simply $y = y_e$ for all x. Of course, this would, in general, not satisfy arbitrary initial data at $x = 0$, but after an adjustment in the western-boundary region described above, it would be anticipated that the outcrop line would seek the constant latitude solution $y = y_e$. The fact that h_3 increases with distance from the eastern boundary forces a longitudinal variation in the outcrop line. From (4.15) and (4.16), we see that the relative variation of h_3 depends on the parameter A. Hence, increased Ekman pumping or a decrease in the layer thickness at the eastern boundary would accentuate the effect described above.

Figures 5 and 6 show the outcrop lines obtained by numerically integrating (4.13) from the western boundary. In these calculations, we have chosen $a = 6000$ km, $y_0/\pi = 1000$ km, $\beta = 10^{-13}$ cm s^{-1}, $f = 10^{-4}$ s^{-1} and $d = 60$ m. In Fig. 5, H_3 has been set equal to 400 m. The outcrop lines for two different relaxation times are shown. The (a) lines are for the case $\kappa^{-1} = 250$ days which yields a value of $r = 0.970$ with the above parameters, while the lines marked (b) refer to the case where the relaxation time has been doubled, i.e., $\kappa^{-1} = 125$ days. The former corresponds to $r = 0.970$, the latter to $r = 1.94$. In each case we have fixed $y_e = 0.75$. Thus, the equilibrium line Y would be different in the two cases and
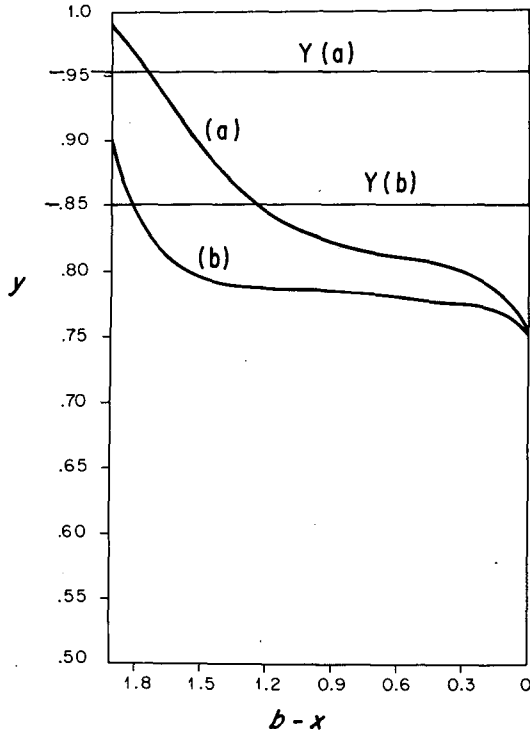
FIG. 5. The outcrop lines calculated from (4.13). Line (a) corresponds to a relaxation time κ^{-1} of 250 days while line (b) has $\kappa^{-1} = 125$ days, $y_e = 0.75$. Y(a) and Y(b) are the latitudes the outcrops would achieve in a resting ocean, $H_3 = 400$ m.

these are labeled Y(a) and Y(b) in the figure. We have also chosen a larger starting value for $y(x)$ in the case of the longer relaxation time. Our reason was twofold. First, we wanted simply to separate the lines initially, but, in addition more substantially, our presumption was that, if the thermal relaxation time was longer, the western-boundary current would tend to carry the isopycnals farther northward.

The boundary layer behavior remarked upon earlier is notable, especially for the larger-r case (b). In addition, the case with larger r displays a smaller southward departure from the equilibrium line. Generally, over the eastern portion of the gyre the north-south slope of the surface isopycnals is less pronounced than in the western half of the gyre.

In Fig. 6 all parameters have been kept fixed except for H_3 which has been doubled to 800 m. The same trend with κ is observed. However, the longitudinal variation of the outcrop line is far less marked. This is in accord with our earlier remarks, i.e., as H_3 increases, A decreases and the *relative* variation of h_3 across the gyre is less and this, in turn, leads to a weaker variation of the outcrop line with longitude.

Figure 7 shows the calculated outcrop line if y_e lies in the southern half of the subtropical gyre. In this case, (4.13) is integrated *westward* from $x = b$. This is consistent with our physical intuition that now y_W is the western latitude of the isopycnal in the formation

region of the western-boundary current. Therefore, we expect that y_W will be specified by the midocean flow rather than the boundary-current flow. The curve (a) in Fig. 7 corresponds to $H_3 = 400$ m and $\kappa^{-1} = 500$ days. The curve (b) corresponds to $\kappa^{-1} = 250$ days but, more importantly, it shows what happens if the outcrop line lies in the region where the Ekman velocity is *northward* and where it dominates the geostrophic meridional velocity which is still southward. Note now that the outcrop line lies *northward* of the equilibrium line (and more northward to the west where the southward geostrophic velocity is less). This implies a *cooling* of the ocean by the atmosphere. These results are consistent with the observational study of Behringer and Stommel (1981) which also found evidence for cooling in the tropical North Atlantic due to the northward advection of warm water by the Ekman wind drift.

5. The thermocline solution south of the outcrop line

Once the outcrop is determined, the circulation south of the outcrop line can be found by the combined use of potential vorticity conservation for layer 3 and the Sverdrup transport relation. The basic idea is described in detail in LPS and just a sketch of the method is given here. The fact that the outcrop line is no longer at constant y (or f) is the only novel feature of the analysis.

For the region south of the outcrop line, potential vorticity in layer 3 (f/h_3) must be constant on geo-
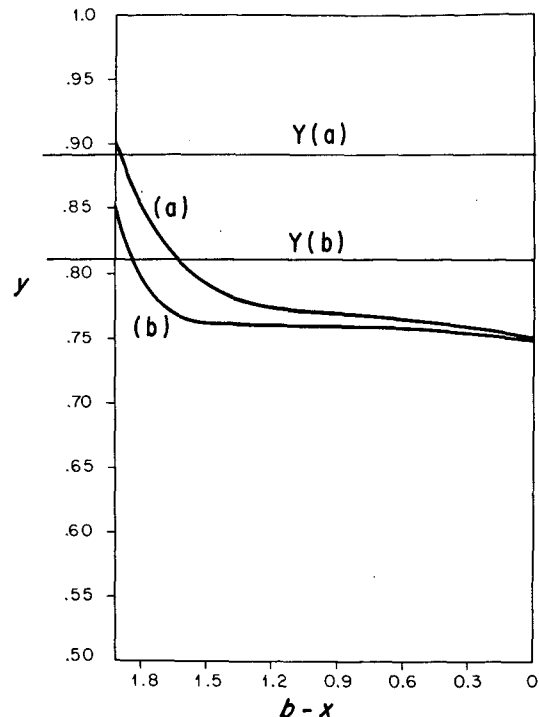

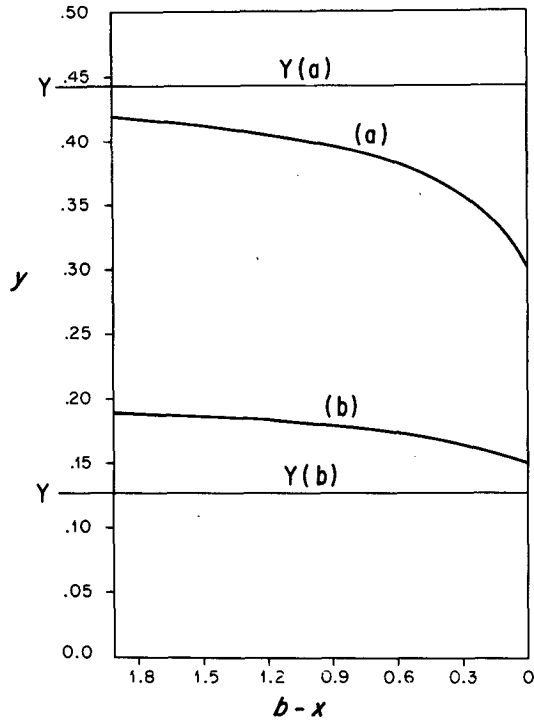FIG. 6. As in Fig. 5 but for $H_3 = 800$ m.

FIG. 7. The outcrop lines when when (a) H_3 = 400 m, κ^{-1} = 500 days and y_e = 0.3, (b) H = 400 m, κ^{-1} = 250 days and y_e = 0.15. Note that (b) implies cooling of the ocean.

strophic streamlines which themselves coincide with the isolines of total depth, $h = h_3 + h_2$. Thus,

$$\frac{f}{h_3} = G(h). \qquad (5.1)$$

But on the outcrop line, $y_2 = y_2(x)$, h_2 vanishes so that h_3 and h are identical there. Also, on the outcrop line f is a function of $y = y_2(x)$. However, since h is a monotonically increasing function of distance from the eastern boundary, f may be considered a function of h along the outcrop line. If we call that function $f_2(h)$, then it follows that (5.1) implies

$$\frac{f}{h_3} = \frac{f_2(h)}{h}, \qquad (5.2)$$

or

$$h_3 = \frac{f}{f_2(h)} h, \qquad (5.3a)$$

$$h_2 = [1 - f/f_2(h)]h. \qquad (5.3b)$$

The Sverdrup transport condition may be written, as in LPS,

$$h^2 + \frac{\gamma_2}{\gamma_3} h_2^2 = D_0^2(x, y) + H_3^2, \qquad (5.4)$$

where D_0^2 is given by (4.5) and $\gamma_2 = g(\rho_3 - \rho_2)/\rho_0$.

The application of (5.3b) yields an equation for the total thermocline depth h, viz.

$$h^2 \left[1 + \frac{\gamma_2}{\gamma_3} [1 - f/f_2(h)]^2 \right] = D_0^2(x, y) + H_3^2. \qquad (5.5)$$

If the outcrop line were a line of constant latitude, $f_2(h)$ would be a constant and (5.5) would be identical to the expression given in LPS. In the present case $f_2(h)$ is determined by the position of the outcrop line which is determined numerically; hence, an analytic expression for $f_2(h)$ is not available. However, the desired information can be easily obtained as follows. We know the variation of h along the outcrop line from (4.15). That is, given a point (x, y) on the outcrop line where $h = h_3$, we can determine h. We evaluate f_2 at this point by writing

$$f = 2\Omega \sin \frac{y}{R},$$

where R is the earth's radius (scaled by y_0). Then the left-hand side of (5.5), which depends only on h and f becomes a function only of f or y for the chosen h. That h-contour may be then traced southward into the subtropical gyre by the application of (5.5) which yields the trajectory

$$x = x(f, h)$$

for each h.

Figure 8a shows the outcrop line and the contours of constant h for the case κ^{-1} = 500 days, H_3 = 800 m, y_e = 0.55, y_W = 0.7 and $\gamma_2 = \gamma_3$ = 0.5. All other parameters are as given before. These correspond to r = 0.97, A = 3.75 and yield Y = 0.756. Contours of selected values of h are shown in the first panel. The contour corresponding to h = 2.03 is just tangent to the outcrop line at $b - x$ = 1.8. There are no ventilated streamlines in layer 3 west of this critical contour. This corresponds to the western-pool region described in LPS. However, while the pool region in LPS was completely girdled by an isoline of potential vorticity, this is not the case here. Although the trajectory emanating from the outcrop has a constant value of f/h, the potential vorticity along the outcrop west of the point of tangency is generally increasing with distance along the outcrop. This is illustrated in Fig. 8b which shows the variation of potential vorticity along the outcrop. The point P is the tangent point, west of which no streamlines enter to ventilate layer 3. It remains somewhat obscure to us how to fill in this pool region. One possibility is to continue the solution (5.5) into the region west of the outcrop where fluid is flowing northeastward across the outcrop (i.e., where layer 3 is exhausted rather than ventilated) and reserve the zone within the westward extension of the h = 2.03 contour for potential vorticity homogenization. We have not pursued such speculations further in this paper.
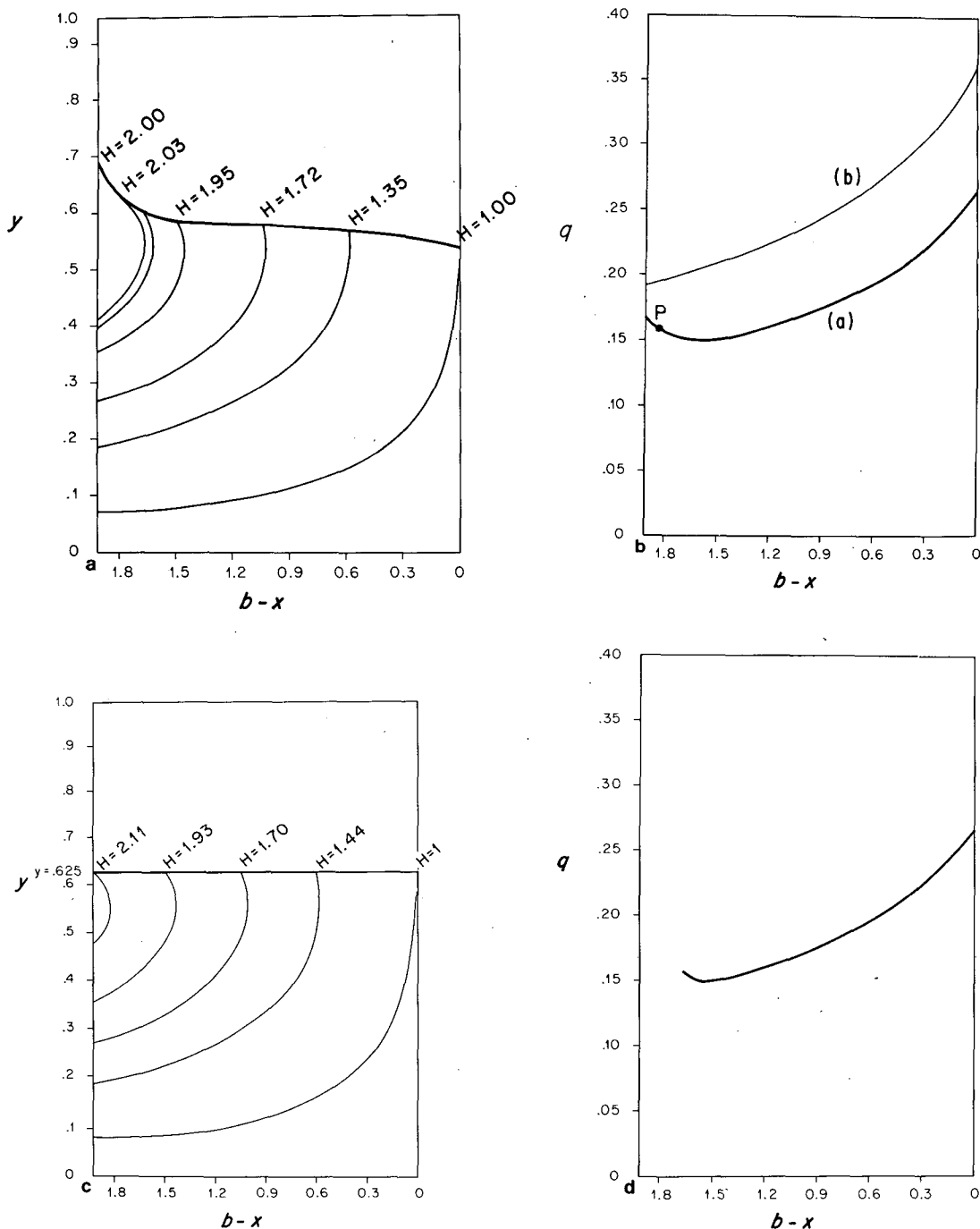
FIG. 8. (a) The outcrop line and streamline pattern (lines of constant h) in the ventilated layer for H_3 = 800 m, κ^{-1} = 500 days; (b) the potential vorticity (a) along the outcrop line and (b) along the line $y = Y$; (c) as in (a) but for a case where the outcrop line is at constant y; (d) the potential vorticity along the line $y = 0.55$.

Figure 8c shows the streamline pattern for the ventilated layer for the case where the outcrop line has been chosen to be a latitude circle at the median between y_W and y_e, in this case at $y = 0.625$. This is similar to the method of latitude averaging used in LPS, and it is of interest to compare the two calcu-

lations. It is evident that over much of the gyre the patterns are very similar. There is simply not sufficient distortion of the outcrop line from the median latitude to affect significantly the ventilated flow. The eastern shadow zone, i.e., the stagnant zone east of the h = 1.0 contour is slightly reduced in the case of the

variable outcrop line simply because the intersection of the outcrop line is swept southward of the median line. More significantly, it is clear that since the outcrop line lies farther northward on the western side of the gyre in the variable case, the unventilated pool has become somewhat larger due to this shift. Recall that the position of y_W is arbitrary in this model and simply reflects the unknown advective effect of the western boundary current. It is immediately clear that one of the greatest influences the western boundary current can have on the dynamics of the ventilated thermocline is in setting the starting position of the surface isopycnals on the western side of the subtropical gyre. The more the boundary current can sweep the isopycnal northward above the median latitude (or the equilibrium latitude) the larger will be the western pool of unventilated water in the western part of the gyre.

It is of interest to return to the question of the potential vorticity variation along the outcrop line. The line (a) in Fig. 8b is the potential vorticity along the calculated outcrop line. As noted above, it has a minimum at about $(b - x) = 1.7$. The increase west of the minimum is due to two factors. As the outcrop line trends northwestward, f increases and the increase in h_3 due to westward displacements (4.15) begins to be offset by the tendency of h_3 to decrease as y moves toward the northern boundary of the gyre. These two factors offset the tendency for the potential vorticity simply to decrease along the outcrop line from east to west, which is what would occur if the outcrop line were a line of constant y. Line (b) in Fig. 8b shows the potential vorticity variation along the line $y = Y$, which, were it an outcrop line, would show a monotonic decrease to the west. Since the potential vorticity is conserved along streamlines, the minimum observed in f/h_3 along the outcrop will be advected into the ventilated region and will show up as a minimum of f/h_3 in longitude along those latitude circles that are crossed by streamlines emanating from both sides of the point of minimum f/h_3 on the outcrop line. This will not be true of all latitudes south of the outcrop. A glance at Fig. 8a shows that lines of constant y in the southern portion of the gyre are ventilated entirely by streamlines emanating from the eastern fraction of the outcrop line, along which the potential vorticity is monotonically decreasing westward. Fig. 8d shows the potential vorticity along the line $y = 0.55$ which is far enough north to contain streamlines from the full span of the outcrop line. Note the minimum of potential vorticity at $(b - x)$ ~ 1.6, i.e., displaced eastward of the position of the minimum on the outcrop line. Note that the graph terminates west of the bounding streamline of the unventilated zone beyond which the potential vorticity is undetermined in our solution.

Figure 9 shows another example in which κ^{-1} = 250 days, H_3 = 400 m, y_e = 0.55 while y_W = 0.75.

In Fig. 9a we have shown the outcrop line and the ventilated streamlines. Fig. 9b shows the ventilated streamlines if the outcrop latitude is chosen to be the atmospheric equilibrium line $Y = 0.738$. Again, over most of the gyre the streamline pattern is very similar. There is, again, a slight reduction in the size of the eastern shadow zone in the variable outcrop case. Note, however, that the western unventilated pool is slightly decreased in size in the case of the variable outcrop even though its latitude at the western boundary, y_W, is greater than Y. This is simply due to the tangent h contour, i.e., 3.57, emanating from a more southerly point than the h contour that emanates from the intersection of Y with the western boundary in Fig. 9b. Generally, however, the larger y_W is, the larger the unventilated western pool. Figure 9c shows perhaps an extreme example where y_W is 0.95, H_3 = 400 m and κ^{-1} = 500 days. A large part of the gyre now cannot be ventilated from the outcrop line.

Figure 9d shows the calculated potential vorticity for the circulation shown in Fig. 9b. The (a) line is the potential vorticity along the outcrop line. Again, a minimum is observed towards the west. The (b) line shows the potential vorticity along the line y = 0.55. The minimum (which again lies eastward of its image on the outcrop line) is barely achieved before the unventilated zone is crossed. Line (c) is the potential vorticity along a more southern latitude line, y = 0.30, and no minimum is seen since all streamlines crossing this line emanate east of the potential vorticity minimum on the outcrop line.

6. Discussion

We have described a simple mixed layer model coupled to a ventilated thermocline. We are well aware of the inadequacies of our mixed layer model, chief among them being our use of a spatially constant mixed layer depth and our presumption that the long-term averaged effect of the mixed layer can be modeled by a steady state description of the mixed layer. The removal of these inadequacies is clearly a goal for future work, and it would not be helpful for us to attempt to speculate what effects this would have on the results of the present study.

The results we have found are rather striking and, in retrospect, easily understood. The surface density field is generally strongly affected by advection. This effect is greater in the northern portion of the subtropical gyre than in the southern part since in the north, meridional geostrophic advection reinforces the southward wind drift, while in the southern part, they are in opposition.

The implicit role of the western-boundary current is seen to be important in setting the entry conditions for the surface isopycnals in the northwest part of the gyre. Within a scale $r^{-1}y_0$, the outcrop line tends
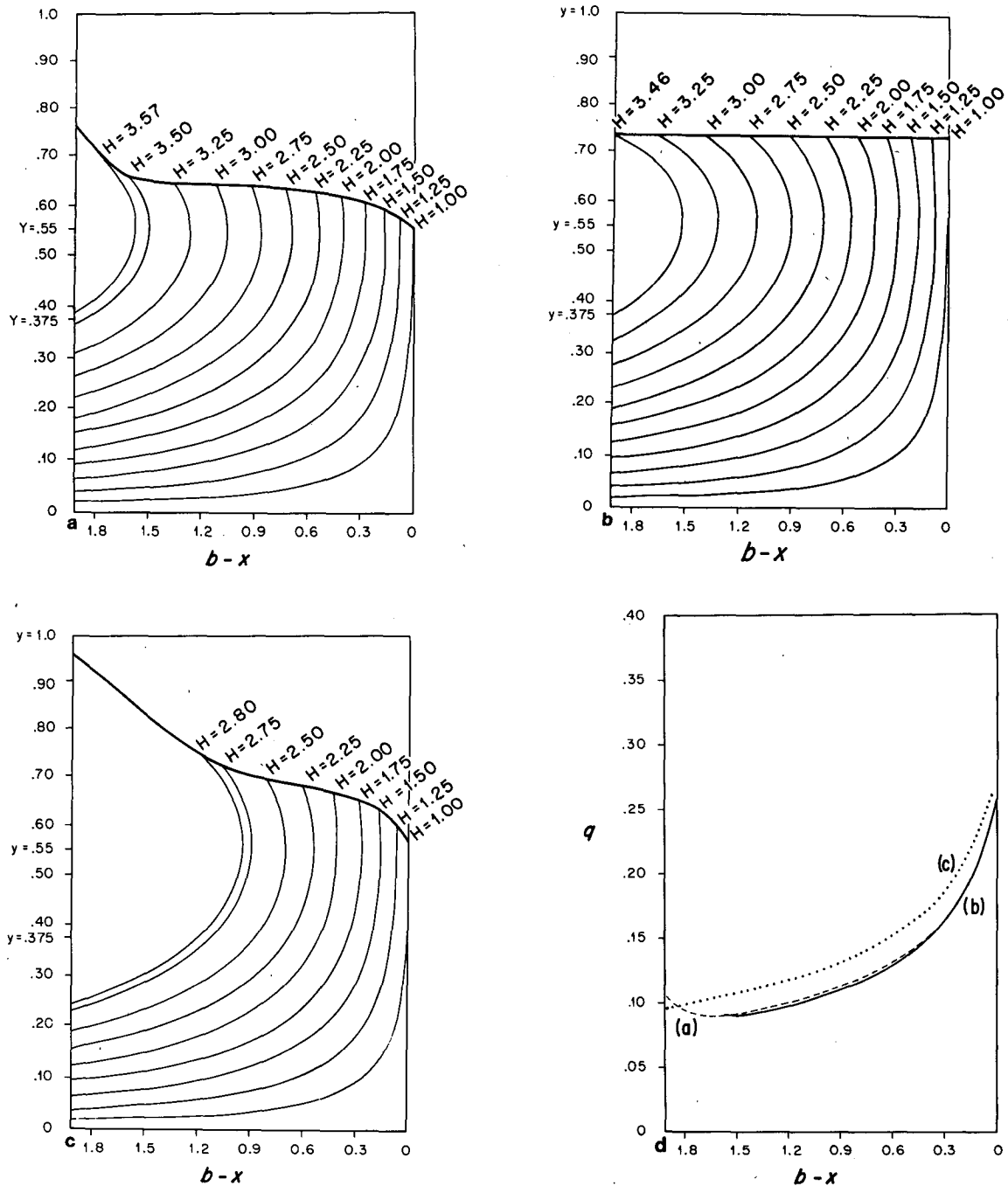
FIG. 9. (a) The outcrop line and streamline pattern for $H_3 = 400$ m, $\kappa^{-1} = 250$ days, $y_e = 0.55$ and $y_W = 0.75$; (b) as in (a) but for the outcrop line at $y = Y$; (c) the outcrop line and streamline pattern for $H_3 = 400$ m, $\kappa^{-1} = 500$ days, $y_e = 0.55$ and $y_W = 0.95$; (d) the potential vorticity for the flow in (a): (a) along the outcrop line, (b) along $y = 0.55$ and (c) along $y = 0.3$.

more or less to a constant latitude line. This line is shifted south of the zero-heating line in the northern part of the gyre. The reverse holds true in the southern portion. Hence, in our model the northern part tends to be heated by the atmosphere, while the southern part is cooled.

The circulation patterns we have calculated in the ventilated layer south of the outcrop line are qualitatively similar to the pattern in LPS which used outcrop lines at constant latitudes. The major qualitative change is the role of the latitude of the outcrop on the western boundary. We believe this parameter

is set by the northward advection by the western-boundary current beyond the latitude which would be fixed by the atmospheric temperature. Roughly speaking, the farther north the outcrop line is dragged by the boundary current, the larger the unventilated western pool will be.

Since the outcrop lines are no longer latitude circles, the possibility now arises that the potential vorticity need not monotonically decrease to the west along outcrop lines. Instead, a minimum appears at some longitude and this is swept into the ventilated zone. Thus, at some latitudes south of the outcrop, the potential vorticity will show a minimum as a function of longitude. However, at great distances from the outcrop in the southern portion of the gyre, the fluid is ventilated primarily from the eastern end of the outcrop and the potential vorticity again displays a monotone character as in LPS. This raises the possibility that the nature of the potential vorticity *variation,* as opposed to its magnitude, might provide a useful diagnostic for the determination of the sources of the ventilated layers.

We also believe it would be of interest to consider models with more than one outcrop line in order to determine the cumulative effect of advection on the surface density field and the thermocline structure. This problem is considerably more complicated tech-nically (although identical in principle) than the problem we have described here. The primary difficulty is that now, south of the first outcrop line, we no longer have analytic representations for the geostrophic velocity, which renders the solution of (2.14) more intricate. This problem is being considered.

REFERENCES

Behringer, D. W., and H. Stommel, 1981: Annual heat gain of the tropical Atlantic computed from subsurface ocean data. *J. Phys. Oceanogr.,* **11,** 1393–1398.

de Szoeke, R. A., 1980: On the effects of horizontal variability of wind stress on the dynamics of the ocean mixed layer. *J. Phys Oceanogr.,* **10,** 1439–1454.

Levitus, S., 1982: *Climatological Atlas of the World Ocean.* NOAA Prof. Pap. No. 13, U.S. Govt. Printing Office, 173 pp.

Luyten, J. R., J. Pedlosky and H. Stommel, 1983: The ventilated thermocline. *J. Phys. Oceanogr.,* **13,** 292–309.

Niiler, P. P., 1975: Deepening of the wind-mixed layer. *J. Mar. Res.,* **33,** 405–422.

Pedlosky, J., and W. R. Young, 1983: Ventilation, potential-vorticity homogenization and the structure of the ocean circulation. *J. Phys. Oceanogr.,* **13,** 2020–2037.